Seismic Analysis of the Stylite Tower at Umm ar-Rasas

Paolo Clemente[1(✉)], Giuseppe Delmonaco[2], Lucamaria Puzzilli[2], and Fernando Saitta[1]

[1] ENEA, Casaccia Research Centre, Rome, Italy
{paolo.clemente, fernando.saitta}@enea.it
[2] ISPRA, Department for the Geological Survey of Italy, Rome, Italy
{giuseppe.delmonaco, lucamaria.puzzilli}@isprambiente.it

Abstract. A seismic vulnerability analysis carried out on the Stylite Tower at Umm ar-Rasas, Jordan, which is a UNESCO World Heritage Site, is presented in this paper. The monument, a unique survived example of stylite towers in the Middle East, presents evidence of structural damage due to earthquakes. The study was based on preliminary investigations, which consisted in Schmidt-hammer tests executed on stone blocks and passive tromography tests on the ground. Two models were implemented for the tower. In the first one, the tower was considered as a rigid structure supported by means of an elasto-perfect plastic cushion at the base. In the second one, a finite element model was setup, with solid elements characterized by a Drucker-Prager yield criterion. In both cases a push over analysis was performed, which resulted in a very low resistance of the tower to seismic actions. The work is part of a preservation effort which will include the design of a retrofit intervention.

Keywords: Masonry tower · Stylite tower · Stability of towers
Seismic behavior of towers · Push over analysis

1 Introduction

The Stylite Tower of Umm ar-Rasas was built in the first half of the 6th century A.D. The tower is 13.5 m tall, with a square base of side $b = 2.52$ m. On the external surface 35 rows of trimmed local limestone blocks laid dry are visible (Fig. 1a). A rectangular hole of about 30 cm × 40 cm size, eccentrically placed, is the only void in the cross section, for most of the height of the tower. It presents also a small chamber at the basement, which reduces remarkably its effective cross-sections. Some of the external blocks are laid to provide a connection with the internal fill, made of rubble masonry of similar material. The masonry tower is founded on a concrete slab, directly placed on the bedrock, with the same size of the tower base section and thickness of about 40 cm. Some of the stone blocks are cracked, especially those on the base layer; furthermore, some blocks located at different heights show relative displacement and the resulting space between them has been recently filled with stone slabs. The limestone blocks are also affected by different nature and degree of weathering. According to the available

R. Aguilar et al. (Eds.): *Structural Analysis of Historical Constructions*,
RILEM Bookseries 18, pp. 1780–1788, 2018.
https://doi.org/10.1007/978-3-319-99441-3_191

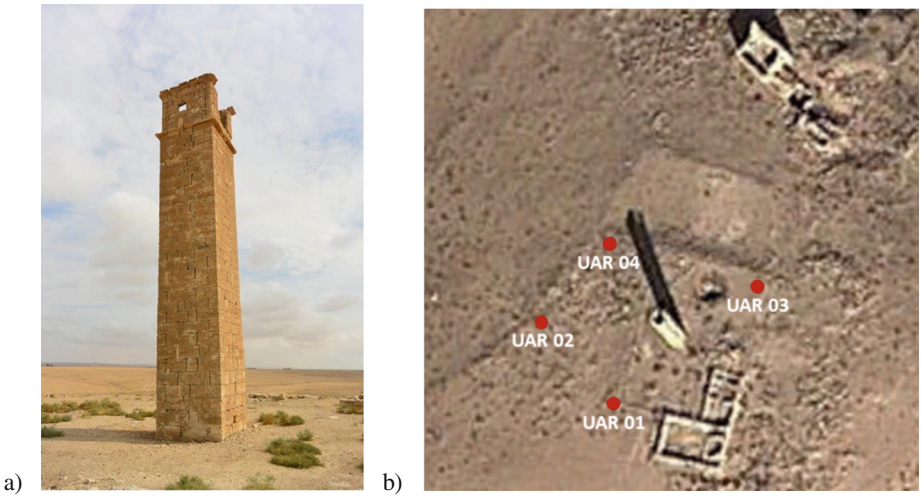

Fig. 1. (a) The Stylite Tower at Umm ar-Rasas, and (b) position of passive tromography tests UAR01-UAR04

sources [1], the Tower was heavily damaged by a strong earthquake occurred in 759 A. D., which caused the failure of the upper part of the structure originally covered by a dome and a vaulted roof. The most recent destructive seismic event that affected the area was the Jericho earthquake, occurred on July 11th, 1927 (Ml = 6.2), which caused heavy damage in the close cities of Salt, and Amman. The earthquake probably caused damage also to the Stylite Tower, due to its vicinity to the epicenter [2, 3]. According to the Jordan seismic map the area is characterized by high seismicity [4, 5], with a peak ground acceleration of 0.2 g, and a structural amplification of 2.5.

Based on previous studies on masonry tower structures [6–9] and other monumental structures [10, 11], the seismic vulnerability of the tower has been evaluated in the framework of the preservation effort, which will include the design of a retrofit intervention.

2 On-Site Investigations

The area of Umm ar-Rasas is characterized by the presence of the Al-Hisa Phosporite formation (Campanian-Maastrichtian), 55–65 m thick [12–15], and, in particular, of the Bahiya coquina member, from few meters to 30 m thick. The blocks forming the stylite tower are made of the same material excavated in an old quarry located near the structure. Boreholes and laboratory tests on rock materials were performed in November and December 2009 [16]. Successively, between 2014 and 2015, some experimental analyses were carried out on the tower and the limestone rock. Schmidt-hammer tests on stone blocks for in-situ assessment of the Uniaxial Compressive Strength (UCS) of the tower limestone material, and four passive tomography tests for

a field evaluation of the dynamic resonances of the soil/bedrock and tower structure were executed.

The analysis of UCS was carried out on thirty-one stone blocks forming the first three external base rows of the tower. On each block, a mechanical test using L-type Schmidt Rebound Hammer was performed following the reference standards proposed by ISRM [17] and ASTM [17]. A total of 310 measurements of rebound values on 31 limestone blocks were considered for the analysis. The same values were classified according to rock strength classes proposed by ISRM (1978), in order to provide a general view of the rock quality for any block analyzed.

According to the results obtained, about 6% of the samples are in R2 class, 58% and 34% are in R3 and R4 classes, respectively. A total of twenty-nine limestone blocks analyzed present a medium-high strength value and are coherent with UCS values obtained by laboratory analysis for intact limestone blocks of Al-Hisa Phosphorite formation [18]. The lower values of UCS are mainly due to the high weathering conditions and presence of cracks, which affect the limestone material mostly concentrated in the NE corner of the structure.

Horizontal to Vertical Spectral Ratio technique (HVSR) at the site was performed using the Micromed's tromograph "Tromino®" equipped with three orthogonal electrodynamic velocimeter sensors and an internal GPS antenna. Measurements were done at four positions in the vicinity of the tower in order to provide information on possible stratigraphic amplification and/or about the dynamic interaction of the structure with the soil (Fig. 1b) [19]. Tests lasting 20 min were carried out with a sampling rate of 128 points/s. Ambient noise was recorded and analyzed with "Geopsy", an open source software used for geophysical research and applications (ver. 2.9.0). By applying the spectral ratio technique, an average H/V curve was retrieved for each site, as well as the spectral ratios N/V and E/V between the single horizontal components (N for NS direction; E for WE direction) and the vertical component of the motion for each location.

A very small amplitude of the signals results from the analysis of the whole spectra. This outcome is coherently related with a low densely populated area such as Um-ar-Rasas, that is far from usual sources of anthropogenic noise (e.g. traffic, industrial activities). On the other hand, this situation resulted in records of ambient noise, whose elaboration via HVSR technique is useful to detect the frequency peaks that can be considered a good preliminary estimate of the fundamental resonance frequency of the site.

Data elaboration highlighted the presence of two distinct ranges of frequency peaks. The first range is between 1.0 and 2.5 Hz and can be quite clearly detected in all the observed positions and curves except N/V for the positions UAR01 and UAR04. The second range is between 4.0 and 6.0 Hz. A clear directionality of the H/V peaks has been detected, more evident at UAR02 and UAR03 positions. As a final result, the recording sites are close to the Stylite tower whose foundations were built directly on the limestone bedrock that largely outcrops in the surrounding area. For this reason, the frequency peaks are not due to the site stratigraphy, but probably are induced on the ground by the tower.

3 Push Over Analyses

3.1 Present Configuration

The experimental analysis described above has demonstrated that the limestone blocks present very dispersed values of the strength, with lower values mostly concentrated in the North and East walls. Taking into account the lack or bad quality of the mortar, the irregularity of the joints, the absence or non-effectiveness of the transversal connections, a reasonable value of the UCS of the tower masonry is in the range of 5÷10 N/mm^2, and the corresponding Young's modulus is between 5000 and 10000 N/mm^2 [20, 21]. The lower limit values are considered in the following; $\hat{N} = W/N_0 = 0.051$ for compression strength $f_m = 5.0$ N/mm^2 (where $N_0 = b^2 f_m$, and b is the side of the square base). The tower total weight is $W = 1{,}800$ kN, with an eccentricity $e_w = 0.021$ m, along the straight line r (Fig. 2), considering the basement and the original dome/vault structure. As a result, the cross section is all effective and the maximum value of the stress is much lower than the allowable one. Therefore, the hypothesis of a linear elastic behavior for the interface section in the present configuration is correct.

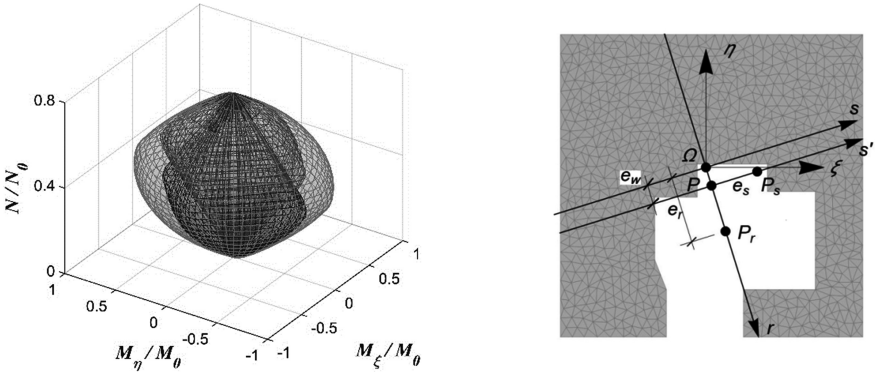

Fig. 2. Limit surfaces LS1, LS2 and LS3 of the cross-section S2.

Two types of analysis were performed, (a) assuming a rigid structure supported by means of an elasto-perfect plastic cushion at the base and (b) implementing a finite element model, respectively. The reason for this approach is given by the geometry of the tower and the mass distribution along the height, which suggests that under horizontal loads yielding occurs first in the void section at the basement. Therefore, the simple rigid model (a) with concentrated plasticity could give a good estimate of the seismic capacity of the tower taking easily into account the directionality of the seismic input, by construction of the three-dimensional limit surface of the critical section. The second model does not suffer the limitations of the first one, being based on solid finite elements capable of yielding, with a Drucker-Prager criterion for three-dimensional stresses, suitable for the masonry of the tower.

3.2 Rigid Model

Figure 2 shows the three limit domains of the base cross-section, related to the following limit states: (i) compression stress equal to zero at one edge (limit state LS1); (ii) compression stress equal to f_m at one edge (limit state LS2); (iii) effective cross-section uniformly compressed with stress equal to f_m (limit state LS3). In Fig. 3, M_ξ and M_η are the bending moments normalized with respect to $M_0 = b^3 f_m/8$, i.e. the maximum bending moment for the square cross-section. Consider the oriented straight line r, passing through the gravity centre Ω of the cross-section and the actual stress point P and suppose that the eccentricity increases along r (Fig. 2). Given the mass along the height of the tower $m(z)$, if the increment of the eccentricity is related to a horizontal seismic acceleration $a(z)$, linearly increasing with the height, the relation between the ratio F/W (between the horizontal resultant F applied at height z_F and the weight W applied at center of mass, whose height is z_W) and the rotation α at the base (the eccentricity e is a function of α):

$$F/W = (e - z_w \cdot \alpha)/z_F \tag{1}$$

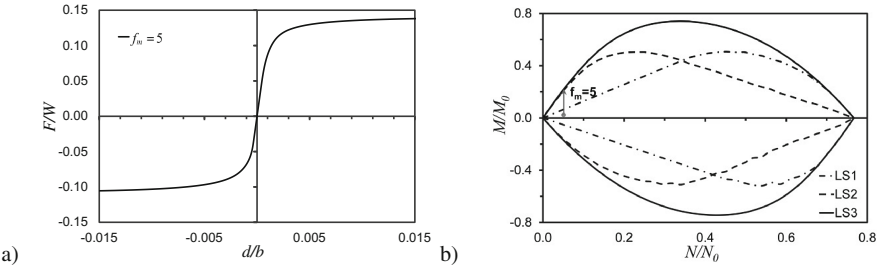

Fig. 3. Force – displacement curve for the rigid model (a) and section of the limit domain (b) at loading path plane (gray arrow).

In Fig. 3a, the characteristic curve F/W versus the generalized displacement d (b is the side of the square base), which can be deduced as the ratio between the work L of the external load related with displacements $d(z)$ and the generalized force F:

$$d = L/F = \int_0^H m(z) \cdot a(z) \cdot d(z) \cdot dz \Big/ \int_0^H m(z) \cdot a(z) \cdot dz \tag{2}$$

is plotted for f_m = 5.0 N/mm^2 and E = 5000 N/mm^2, for the case of eccentricity increasing along the direction r. As one can see, the maximum value of F/W, which represents the horizontal acceleration, is very low if compared with the acceleration spectral amplitudes at the site.

The section of the surface of Fig. 2 is represented in Fig. 3b for the considered case with constant eccentricity. The loading path, in terms of the moment at the basement, is shown by an arrow.

3.3 Elastic-Plastic Model

A Finite Element model was set up using Ansys® computer code. SOLID65 elements were used and the tower was supposed to be fixed at its basement. The modal analysis provided the first three frequencies, reported in Table 1. The first modal shape presents prevalent displacements along *y* axis, while the second modal shape has prevalent displacements along *x* axis. The third mode is torsional; the higher modal shapes are similar to the higher modes of a cantilever.

Table 1. Numerical frequencies (y and x are parallel to η and ξ, respectively).

Mode	1	2	3
f (Hz)	3.42	3.54	16.13
Prevalent motion	y	x	Torsional

After the analysis of the different models presented in literature, an elastic - perfect plastic behavior was assumed for the masonry, and the Drucker-Prager limit domain for three dimensional stress states, which is a smooth version of the Mohr-Coulomb criterion, was adopted. Reasonable values of cohesion and friction coefficient are $c = 0.1$ N/mm^2 and $\mu = 0.6$, respectively [22]. Zero value for the dilatancy was assumed.

Two pushover analyses were carried out, by applying an incremental distribution of nodal forces according to the inertial forces of the first and the second modal shape (i.e. $\pm\mathbf{m}\phi_i$ where **m** is the mass matrix and ϕ_i the i-*th* modal vector), respectively (Fig. 4), and plotting the force – displacement curves of the equivalent single degree of freedom elasto - plastic oscillators.

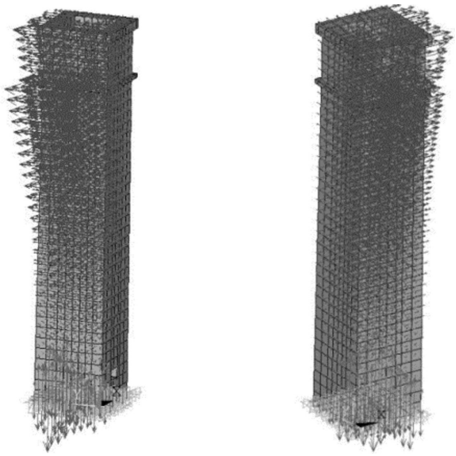

Fig. 4. Nodal forces for nonlinear static analysis according to the first mode and the second mode.

In Fig. 5 the force-displacement curves for c = 0.1 N/mm^2 and μ = 0.6 are plotted, for force distribution simulating mode 1 and mode 2, respectively. The non-symmetric resistance for forces simulating mode 1 (prevalent forces along y direction) is apparent, due to the absence of symmetry in the section at the base of the tower. The difference for mode 2 (prevalent forces along x direction) is less evident. In all the cases the seismic capacity is very low with respect to the seismic demand requested by the code. This latter, with reference to the cases represented in Fig. 5a, is equal to 0.011 (positive) or 0.019 (negative), whereas for the case in Fig. 5b is 0.015 (positive) or 0.013 (negative). Figure 6 show the plastic strain intensity at collapse for the first case and highlights as the plastic strain is effectively concentrated at the walls of the base chamber, whereas the remaining part of the tower remains in the elastic range. This is consistent with the hypotheses assumed in the simplified model of the tower.

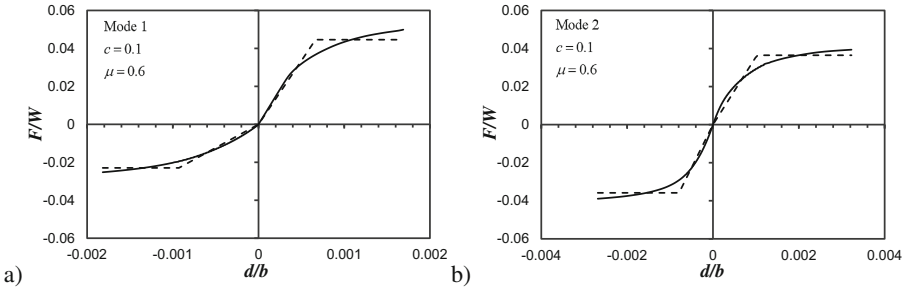

Fig. 5. Force – displacement curves for the elastic model.

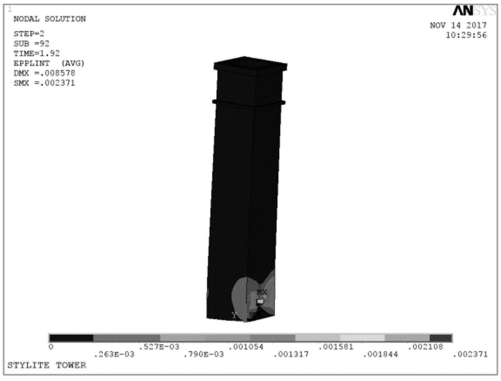

Fig. 6. Plastic strain intensity.

4 Conclusions

The seismic vulnerability analysis carried out for the Stylite tower of Umm ar-Rasas (Jordan) has been presented in this paper. The ground and the structural material were characterized by means of in situ experimental tests and two distinct structural models were implemented.

In the first model, the tower was assumed as infinitely rigid, but supported by an elasto-plastic cushion at its base, whose length is related with the presence of a chamber, which reduces significantly the cross-section area. The domains of the limit states for this section of the tower were numerically derived, evaluating the safety in the present stress state and under eccentricity of the dead load varying along selected straight lines in the cross-section. Assuming the eccentricity as due to a triangular horizontal acceleration diagram, acting along the rigid tower, the characteristic curves generalized force – generalized displacement were plotted with reference to two distinct values of strength and elastic modulus of the masonry. A comparison with the seismic actions, provided by the Jordan code for the site, shows a capacity much lower than the demand.

The second approach was based on a FE model using solid elements, and material characterized by elasto-plastic behavior and Drucker-Prager limit domain for three-dimensional stress states. Three-dimensional load conditions were considered, using forces proportional to the first two modal shapes weighted by masses. Force-displacement capacity curves obtained by incremental static nonlinear analysis for reasonable values of cohesion and friction show a very low performance of the tower under seismic actions. Better results are obtained increasing cohesion over the acceptable level in the actual state of the structure, and with the lower values of friction coefficient, corresponding to more ductile behavior.

Acknowledgements. The paper is part of collaboration between the Department of Antiquities of the Hashemite Kingdom of Jordan (DOA), ISPRA and ENEA and contributes to meeting the requirements of UNESCO World Heritage Center for the conservation of the Stylite Tower of Umm ar-Rasas. The authors are grateful to Prof. Monther Jamhawi (DOA Managing Director) and DOA staff for their continuous support and encouragement.

References

1. Sbeinati MR, Darawcheh R, Mouty M (2005) The historical earthquakes of Syria: an analysis of large and moderate earthquakes from 1365 B.C. to 1900 A.D. Ann Geophys 48 (3):347–435
2. Avni R (1999) The 1927 jericho earthquake. Comprehensive macroseismic analysis based on contemporary sources. Ben Gurion University of the Negev, Beer Sheva (in Hebrew)
3. Zohar M, Marco S (2012) Re-estimating the epicenter of the 1927 Jericho earthquake using spatial distribution of intensity data. J Appl Geophys 82:19–29
4. Menahem AB (1991) Four thousand years of seismicity along the dead sea rift. J Geophys Res 96(B12):20195–20216

5. Thomas R, Niemi TM, Parker ST (2007) Structural Damage from Earthquakes in the Second-Ninth Centuries at the Archaeological Site of Aila in Aqaba. Bulletin of the American Schools of Oriental, Jordan
6. Bongiovanni G, Celebi M, Clemente P (1990) The Flaminio obelisk in Rome: vibrational characteristics as part of preservation efforts. Int J Earth Eng Struct Dyn 19(1):107–118. https://doi.org/10.1002/eqe.4290190110. ISSN 0098-8847.90.010107
7. Buffarini G, Clemente P, Paciello A, Rinaldis D (2008) Vibration analysis of the lateran obelisk. In: Proceedings of 14th World Conference on Earthquake Engineering (14WCEE, Beijing, 12–17 October), Paper S11-055, IAEE & CAEE, Mira Digital Publishing, Saint Louis
8. Clemente P, Saitta F, Buffarini G, Platania L (2015) Stability and seismic analyses of leaning towers: the case of the minaret in Jam. Struct Des Tall Spec Build 24:40–58. 10.1002.tal.1153. Accessed 11 Feb 2014
9. De Stefano A, Matta E, Clemente P (2016) Structural health monitoring of historical heritage in Italy: some relevant experiences. J Civil Struct Health Monit 6(1):83–106. https://doi.org/10.1007/s13349-016-0154-y. Accessed 23 Feb 2016
10. Bongiovanni G, Buffarini G, Clemente P, Rinaldis D, Saitta F (2017) Experimental vibration analyses of a historic tower structure. J Civil Struct Health Monit 7(5):601–613. https://doi.org/10.1007/s13349-017-0245-4. Accessed 16 Oct 2017
11. Bongiovanni G, Buffarini G, Clemente P, Rinaldis D, Saitta F (2017) Dynamic Characteristics of the Amphitheatrum Flavium northern wall from traffic-induced vibrations. Ann Geophysics 60(4):S0439. https://doi.org/10.4401/ag-7178. INGV, Rome, Accessed 12 July 2017
12. Bender F (1974) Geology of Jordan. Gebruedre, Berlin. 196 p
13. Tarawneh B (1985) The Geology of A-Hisa (Al I'na). Map Sheet No. 3151-I. Natural Resources Authority, Amman, Jordan
14. Powell JH (1989) Stratigraphy and sedimentation of the Phanerozoic rocks in central and south Jordan. Natural Resources Authority, Geological Mapping Division, Amman. 130 p
15. Sadaqah RM (2000) Phosphogenesis, geochemistry, stable isotopes and depositional sequences of the upper cretaceous phosphorite formation in Jordan. PhD thesis, University of Jordan, Amman. 257 p
16. Azzam M, Doukh F (2009) Site investigation for saint stylite tower at Um er-Rasas/Madaba. Annex 1: Geological report for the Stylite Tower. Technical report, Natural Resources Authority, Amman (Jordan)
17. ISRM (1978) Suggested methods for determining hardness and abrasiveness of rocks. Int J Rock Mech Min Sci Geomech Abstracts 15:89–98
18. Naghoj NM, Youssef NAR, Maaitah ON (2010) Mechanical properties of natural building stone: jordanian building limestone as an example. Jordan J Earth Environ Sci 3(1):37–48
19. Margottini C, Spizzichino D, Sonnessa A, Puzzilli LM (2015) Natural hazard affecting the Katskhi Pillar Monastery (Georgia). Eng Geol Soc Territ 8:393–397
20. Dweirj M, Fraige F, Alnawafleh H, Titi A (2017) Geotechnical characterization of jordanian limestone. Geomaterials 7:1–12
21. Fener M, Kahraman S, Bilgil A, Gunaydin O (2005) A comparative evaluation of indirect methods to estimate the compressive strength of rocks. Rock Mech Rock Eng 38(4):329–343
22. Vasconcelos G, Lourenço PB (2009) In-Plane experimental behavior of stone masonry walls under cyclic loading. J Struct Eng 135(10):1269–1277 ASCE